

Review

# A Brief Review of the Latest Advancements of Massive Solar Thermal Collectors

Alessia Aquilanti <sup>1,2,\*</sup> , Ignacio Peralta <sup>2,3,4,\*</sup> , Eduardus A. B. Koenders <sup>2</sup>  and Giovanni Di Nicola <sup>1,\*</sup> 

<sup>1</sup> Department of Industrial Engineering and Mathematical Sciences, Marche Polytechnic University, Via Breccie Bianche 12, 60131 Ancona, Italy

<sup>2</sup> Institute of Construction and Building Materials, Technical University of Darmstadt, Franziska-Braun-Str. 3, 64287 Darmstadt, Germany; koenders@wib.tu-darmstadt.de

<sup>3</sup> Centro de Investigación de Métodos Computacionales (CIMEC), Universidad Nacional del Litoral (UNL)/Consejo Nacional de Investigaciones Científicas y Técnicas (CONICET), Predio CONICET “Dr. Alberto Cassano”, Colectora Ruta Nac. 168 km 0, Paraje El Pozo, Santa Fe 3000, Argentina

<sup>4</sup> Facultad Regional Santa Fe, Universidad Tecnológica Nacional (UTN), Lavaise 610, Santa Fe 3000, Argentina

\* Correspondence: a.aquilanti@staff.univpm.it (A.A.); iperalta@cimec.unl.edu.ar (I.P.); g.dinicola@univpm.it (G.D.N.)

**Abstract:** Technologies that can contribute to the reduction of greenhouse gases are mandatory, and those based on solar energy are good candidates to achieve this. In this sense, massive solar thermal collectors are suitable technologies for supplying the primary energy demand of buildings. To design these devices, it is necessary to fully understand the physics of the problem before proposing any new optimized solution. This review aims to briefly summarize significant aspects regarding the current state of development of these solar technologies. Attention is paid to works devoted to experimental studies to analyze the behavior of these systems, as well as numerical models to predict the physics of the problem. Furthermore, the future directions and prospects in the field of massive collectors are briefly described. The main novelty of this review is to provide a comprehensive overview that summarizes the works done so far in the field over the past 30 years, which allows the reader to delve deeper into the topic. According to the reviewed works, it can be concluded that these technologies can contribute to the reduction of greenhouse gases while at the same time being excellent examples of the integration of solar energy devices with buildings.

**Keywords:** massive solar thermal collector; solar energy; thermal energy storage; heat exchange; concrete; asphalt



**Citation:** Aquilanti, A.; Peralta, I.; Koenders, E.A.B.; Di Nicola, G. A Brief Review of the Latest Advancements of Massive Solar Thermal Collectors. *Energies* **2023**, *16*, 5953. <https://doi.org/10.3390/en16165953>

Academic Editor: Kian Jon Chua

Received: 21 July 2023

Revised: 5 August 2023

Accepted: 10 August 2023

Published: 12 August 2023



**Copyright:** © 2023 by the authors. Licensee MDPI, Basel, Switzerland. This article is an open access article distributed under the terms and conditions of the Creative Commons Attribution (CC BY) license (<https://creativecommons.org/licenses/by/4.0/>).

## 1. Introduction

Buildings energetically more efficient have become a challenge for researchers and engineers, and the efficient design of them is driven by the urgent need to reduce the emissions of greenhouse gases [1]. It is well known that the building stock consumes more than 30% of the world's total energy and emits nearly 40% of the total CO<sub>2</sub> (direct and indirect). This makes buildings the largest energy consumers in the European Union [2]. The search for technologies that can contribute to the reduction of these emissions is mandatory, and those based in solar energy are good candidates to achieve that. For instance, they can supply the primary energy demand of buildings, and in this sense, solar collectors technologies can be suitable for providing hot water in houses and for space heating [3]. In this direction, one of the most well-known solar technology is the so-called flat plate collectors [4], but with the disadvantage of high investment costs that limit the market's expansion of solar-based systems [5]. To circumvent this, there are two suitable paths, the use of alternative materials in order to produce low-cost solar devices, and the integration of solar systems in the building envelope [6]. In this sense, the last strategy is reflected in the so-called massive solar thermal collectors (MSTCs), which are excellent examples of

this integration. The main characteristic of these systems comes from the term “massive”, which highlights the high heat capacity of the materials used for the fabrication of these collectors. This feature allows the extraction of energy in periods of low (even null) solar radiation, which is an important factor in energy sources with a non-constant supply.

An MSTC could be easily described as an arrangement of tubes embedded in a massive matrix that is exposed to solar radiation and acts as an absorber material. Then, a working fluid running inside those tubes extracts the collected heat, entering with a low temperature, and leaving the device with a higher one. Depending on the fluid, it can be used directly for hot water supply or as a thermal fluid for space heating. The most important parameter of these devices is the absorber material, which should have high thermal conductivity to rapidly conduct the stored heat to the tubes (and consequently to the water), and at the same time, high heat capacity to store the highest possible amount of the incoming solar radiation. One material that complies with these requirements is concrete, which, at the same time, can guarantee low investment costs, a non-difficult maintenance, and, the most important feature, it can be used as a structural element, a very attractive characteristic for the integration of MSTCs in the building envelope [3,7]. These properties make concrete the most chosen candidate material for these solar systems.

The high thermal inertia of these devices modifies completely their behavior in comparison with the typical flat plate collectors. In this sense, the design of an MSTC is not always implicitly guaranteed, mainly because its performance is strongly related with the way the daily thermal cycle of the energy source is exploited. Moreover, if the absorber material is combined with Thermal Energy Storage (TES) systems, like Phase Change Materials (PCMs) to improve its thermal storage capacity, the complexity of these PCM-enhanced systems is increased and an optimized design of the effective properties of the absorber is mandatory [8]. Moreover, weather variables, the emplacement location of the device, and its topology influence the absorber properties, making it important to consider these parameters in an optimum manner. As it can be appreciated, there are many parameters that must be considered in the design of an MSTC, which makes it necessary to fully understand the physics of the problem before thinking of proposing any new design. In this sense, the intention of this review is to briefly summarize significant aspects regarding the current state of development of MSTC technologies. The main focus will be on the latest works after the year 2012, since previous studies are well detailed in the review of D’Antoni and Saro [3]. This time gap includes works studying the use of alternative absorber materials, such as asphalts, ceramics, and new coatings, as well as the inclusion of latent-based TES systems within the absorber matrix, or aluminum wire mesh and iron scraps to increase the thermal conductivity of the systems. The gap also covers the latest models to simulate MSTCs, from simple 2D models up to complete, fully 3D simulations, in which the heat transfer problem over the absorber is coupled with the fluid flow inside the tubes. Moreover, a model that combines computational fluid dynamics with experimental data and an artificial neural network is presented. The novelty of this review is that it provides a detailed summary of the works done so far in the field of MSTCs over the last 30 years. The current work is organized as follows: Section 2 presents all experimental works that analyze the behavior of MSTCs; Section 3 is devoted to the numerical modeling to predict the physics of the problem; Section 4 briefly describes future directions and prospects in the field of massive collectors; and in Section 5 are highlighted the main outcomes that must be taken into account for the study and design of MSTCs.

## 2. Experimental Methods

As it is stated in the introduction, MSTCs seem to be an appealing technology to capture the heat energy from the sun. An interesting characteristic that differentiates these devices from the typical flat solar collectors is that MSTCs have their own structural integrity to withstand external loads, which makes these devices suitable for integration with the building envelope. They can therefore be used in different applications with different shapes and orientations, thus eliminating the need for supporting frames. MSTCs

can be implemented as modular systems with reduced construction costs compared to the costs required to construct traditional collectors and are also easy to use and maintain. The durability of metallic materials, which traditional solar collectors are generally made of, is limited by the threat of corrosion. Concrete, instead, is inherently durable, maintenance-free, and has good thermal storage qualities. For this reason, one of the most important advantages of MSTCs made of concrete is their thermal capacity, which allows them to store solar energy and simultaneously makes it possible to extract heat at those times of the day when solar radiation is scarce. The durability of concrete is also another important advantage, especially for building-integrated systems, where durability is an essential requirement.

There are several criteria for distinguishing and classifying MSTCs, which are:

- Type of end application: heating, cooling, or production of domestic hot water (DHW).
- Use of collected heat: direct or indirect method. The first method occurs when solar energy covers partially or entirely the energy demand to produce domestic hot water and/or internal heating in buildings, or when the collected heat from the MSTC can reduce the internal temperature of the building, thus covering part of the demand for space cooling. The indirect method, on the other hand, occurs when the heat collected by the MSTC is used as a source for a heat generation system, such as a heat pump.
- Degree of integration into the building envelope: MSTCs can be fully integrated into the building (Figure 1a) or into the roof or façades; partially integrated (Figure 1b) and detached from the building (Figure 1c). The latter type includes systems that are completely detached from the building envelope such as, for example, horizontal pavements like road surfaces and driveways, or vertical external walls or prefabricated structures like garden perimeter walls and external garage structures. It is evident that in MSTCs completely detached from the building there is no optimization concerning orientation and inclination of the surfaces to better capture the solar radiation, because they are structures or parts of structures that already have a main function.

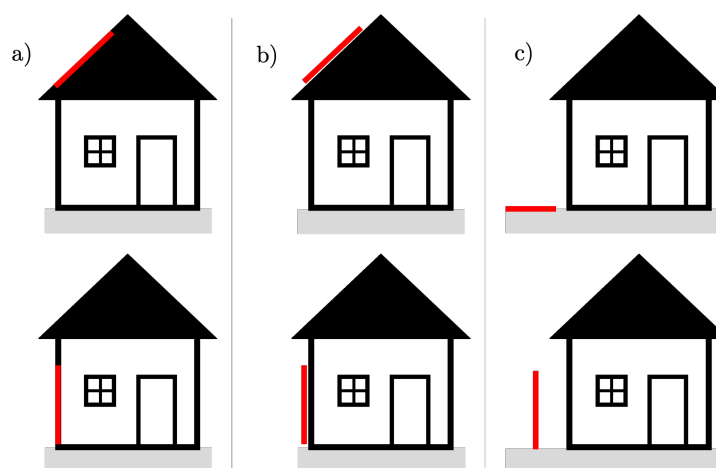


**Figure 1.** Classification of MSTCs (represented by red rectangles) in terms of degree of integration into the building envelope: (a) fully integrated; (b) partially integrated; (c) detached from the buildings.

MSTCs are simple devices to build and are easy to operate. This has motivated a variety of experimental works to study the performance of these systems. In this sense, the following paragraphs aim to describe the main experimental works in the literature. In particular, attention is paid to the various studies carried out after the review by [3] as already specified in Section 1.

Krishnavel et al. [9] made three different types of solar water heaters with concrete absorbers that were tested in parallel, comparing the final performance of each. The three prototypes were constructed using different materials. The first was made of concrete with aluminum pipes incorporated, while the second had PVC pipes incorporated into

the concrete. To increase the thermal conductivity of the system, an aluminum wire mesh and iron scraps were added to the concrete in both prototypes. The third specimen involved concrete and PVC pipes. The experimental campaign was carried out during the period March–May by analyzing different configurations for the position of the collectors: horizontal, at an angle of 18° facing south and at an angle of 30° facing south. The impact on the final performance of the devices on the presence or absence of a green cover was also evaluated. The results showed that only marginal differences in terms of the maximum temperatures reached by the water were recorded in the three prototypes when they were positioned horizontally (65 °C for prototype 1 and 56 °C for prototype 3, both with a green cover). The same results were also recorded for the other two inclinations of the analyzed prototypes. In terms of efficiency, slab 1 at the horizontal position with cover had the highest efficiency of 65%, while slab 3 at 30° inclination facing south and without cover had the lowest efficiency of 30%.

O’Hegarty et al. [10] began investigating the potential of having massive systems in building façades. The authors conducted studies on different building types considering their geometry and functionality. Their preliminary numerical studies showed that there is a linear correlation between solar collector area and hot water consumption. According to the presented data, the proportionality factor can vary between 0.029 and 0.048 m<sup>2</sup> per liters of water (per day). The integration of massive collectors in façades could be a good solution when there is a high demand for hot water but a small roof area of the building. The authors continued the study of this topic by explaining that studies in the literature on non-integrated, roof-attached concrete solar collectors referred to experimental analyses in high-temperature climates and numerical analyses using simplified 1D and 2D models. Therefore, in [11], the authors reported the results obtained from an experimental study on the performance of a concrete solar collector integrated into the building façade for the Dublin location (mid-latitude European climate). In addition, the authors also developed and validated a 3D numerical model of such a system that was used to predict the performance of other building façade-integrated concrete solar collectors for other European climates. In [11], three 0.6 × 0.6 m collectors were manufactured and connected in series: the wooden formwork was made; the copper pipes were first cut and then welded together with the elbows to obtain the final coil; and the heat exchange system was then placed in the formwork and the concrete mixed and inserted into the formwork. To increase the final absorbance of the system, the 3 collectors were painted black and then placed vertically and insulated to simulate a façade installation. The results of the experimental analysis carried out using the 3 massive collectors in series facing south in the Dublin location with a 65 L storage tank showed that the system can provide approximately one-quarter of the annual hot water energy demand of a single occupant dwelling. The results also show that a fair amount of thermal energy can be harvested even in the winter months in contrast to that which can be extracted in horizontally installed collectors.

In the work of Patil et al. [12] the authors, with the aim of reducing the final cost of the solar collector, replaced the metal absorber plate with a concrete absorber plate. The realized collector had dimensions of 2 × 1 m and was tested in different months of the year (September to May) and with different fluid flow rates (20, 25, and 30 L/h). A total of 7 kg of mild steel scrap powder with a diameter of less than 3 mm was added to the concrete mix design to prevent the formation of voids in the concrete slab. A wire mesh was laid over the concrete casting and the copper coil was fixed on top so that half of the coil was embedded in the concrete and the remaining half was exposed to the sun. The wire mesh not only reinforces the concrete slab but also slightly increases the overall thermal conductivity of the system. A layer of dark paint was applied to the surface of the collector. The solar collector was closed with a 3 mm thick plate of glass, forming an air gap of approximately 4 cm inside. During the tests, the collector was mounted on a metal support at an angle of 19° due south. The results of the measurements showed that the concrete collector is capable of supplying the necessary amount of hot water to cover the demand for domestic activities. In detail, during the day, the water leaving the

collector had a temperature between 47 and 57 °C in the rainy season, and between 48 and 59 °C in the winter season, while the temperature recorded in the summer season was between 56 and 80 °C. Furthermore, the authors stated that the concrete collector can be easily integrated into the roof of a south-facing sloping building or into a flat roof, further reducing the installation costs for hot water supply. The reduced costs for the construction of these types of collectors make these devices suitable for rural or remote areas where there is not always a supply of electricity.

In the work of Guldentops et al. [13], the authors studied a pavement solar collector (PSC) with the aim of developing a model of such a system and validating it with a self-instructed experiment. The experimental setup for the validation of the model consisted of a 119 mm thick slab of asphalt concrete, made of two types of asphalt to which copper pipes were embedded. Above the bituminous layer, a grid of copper pipes with an external diameter of 15 mm was placed. The distance between the surface of the plate and the top of the tube was 51 mm. Sixteen thermocouples were placed on the surface and embedded in the asphalt concrete slab in both directions and at different points to know the temperature along the slab at different depths. Through a submersible thermocouple, the temperature of the water leaving the collector was measured. The pavement collector was first left in the sun for about 4 h and, after this time, water started to flow through the pipes. Once the copper pipes were connected through a hose to the water mains, different flow rates were set at preset time intervals starting from 1 L/min up to 4 L/min. The water inlet temperature, measured four times at regular time intervals, varied between 22.1 and 24.1 °C. The experimental results are in good agreement in terms of water outlet temperature and pavement temperature with the developed model.

Sable [14] analyzed the performance of an inexpensive solar collector made of concrete. A wooden frame acted as a container for the concrete composed of metal fibers and for the copper coil, which was half encased in concrete. The addition of the 7 kg of steel fibers was intended to increase the thermal conductivity of the concrete. The upper part of the collector was enclosed by a glass plate. The copper pipes carrying the water had dimples to increase the heat transfer and thus increase the overall efficiency of the collector. The experimental campaign was carried out in different seasons and with different water flow rates in order to evaluate the performance throughout the year. The average water temperature recorded during the day was 59–69 °C depending on the test period. Furthermore, in order to assess and quantify the actual effect of the dimples on the water temperature, two identical concrete plate-collectors, one with a dimpled tubes and the other with smooth tubes, were constructed and subsequently tested in parallel. The results showed that simple tube concrete collectors were able to reach higher outlet temperatures of water than smooth tube concrete collectors (up to 2.5 °C).

Patil et al. [15] studied the feasibility of using concrete as the main material for the construction of a solar collector for hot water storage. The authors designed, fabricated, and tested a 2 m<sup>2</sup> concrete solar collector in Pune, India, covered by a glazed surface, incorporating a copper coil. Tests were conducted in both winter and summer on the concrete collector for different flow rates from 20 to 45 L/h. The results of the experimental campaign showed that the average outlet water temperature was 58 °C, the average overall efficiency of the concrete collector was found to be 34% and its optical efficiency 42.75% while its overall heat loss coefficient was 11.2 W/m<sup>2</sup>K.

Al Hoqani et al. [16] realized a solar collector by replacing the traditional metal frame with concrete reinforced with waste metal fibers. In detail, the selected fibers had a size of 3 mm and were made of copper, mild steel, and aluminium and were added with a volume fraction varying from 0.0011 to 0.0068. Initial tests showed that for the same volume fraction ratio, the final concrete conductivity was much higher when copper fibers were used. For this reason, the authors selected this combination to carry out the other studies. In particular, the effects on the final performance of the massive collector were evaluated with reference to the main design parameters of the collector, i.e., collector thickness, space between the pipes, the mass flow rate of the water and the heat transfer coefficient in terms

of collector efficiency factor ( $F'$ ), diameter of the pipes ( $\varnothing$ ), and heat removal rate ( $F_R$ ). In this sense, the following can be itemized:

- The thickness of the plate affects the performance of the collector. In fact, as the thickness of the collector increases, the efficiency factor and heat removal rate increase, around 47% and 39%, respectively, and tend to become constant with 0.04 m plate thickness.
- As the space between the pipes increases, given constant pipe diameter, overall heat transfer coefficient and fluid flow rate, the heat removal values decrease around 30% and 55%, whatever the plate thickness.
- As the diameter of the tubes increases, the space between the tubes, the water flow rate and the heat transfer coefficient being constant, the fin effectiveness of the collector increases between 4% and 8.9% for all collector thicknesses analyzed. The effectiveness of the collector increases with increasing pipe diameter as the transfer by conduction decreases.
- Given constant pipe spacing and pipe diameter, as the water flow rate increases, the heat reduction factor of the collector increases regardless of the collector thickness.

The results of the analysis showed that the performance obtained with the metal fiber reinforced concrete (MFRC) is comparable to that obtained with a traditional solar collector equipped with metal plates, providing hot water at a temperature of around 50–60 °C with an average daily efficiency of 55–65% and, moreover, thanks to the high thermal lag, the collector would be able to provide hot water even after sunset. The authors stated that this type of collector, integrated in the roof, could offer a good passive solar water heating system and could also be able to reduce the thermal load of the building's cooling systems.

Zaim et al. [17] studied experimentally and numerically a pavement solar collector with the main objective of the analysis being to evaluate the impact of the tube configuration on the thermal dynamics and performance of the PSC. Considering the possible tube configurations that can be incorporated into the collector, the authors analyzed a series of unbalanced ladder shapes, balanced ladder shapes, and parallel configurations. The prototype realized consisted of a wooden container measuring 3 × 0.4 m and 0.2 m in height filled with 3 layers of compact asphalt mixture consisting of 60/70 bitumen, crushed sand, and the minimum possible number of voids. Stainless steel pipes with an internal diameter of 15.8 mm were embedded in series in the middle layer at a depth of 3 cm below the pavement surface at regular intervals and with center-to-center spacing of 110 mm. Expanded polystyrene pipes and glass fiber wool were used to insulate the connections between the steel pipes and the tank in order to reduce heat dissipation. The experimental campaign took place during the day from 9:30 to 16:30 during summer and winter periods, and the water flow rate of 24 L/h was kept constant during the various tests. The results of these tests were used to validate the numerical model: the experimental data sets were used in the model in order to calculate the water outlet temperature. The latter was then compared with the temperature actually obtained from the experimental test, demonstrating the accuracy and robustness of the developed numerical model.

Masoumi et al. [18] studied numerically and experimentally an asphalt solar collector (ASC). The prototype had a surface area of 1 m<sup>2</sup> and inside the slab, three 2 m long galvanized tubes were placed in parallel. After construction, the prototype was buried to recreate ideal conditions in terms of heat transfer with the ground. The experimental campaign was conducted from 9:00 to 17:00 during the months of November and August, and four different water flow rates (0.25 L/min, 0.50 L/min, 0.75 L/min, and 1.50 L/min) were analyzed on four consecutive test days. During the tests, the inlet water temperature was a constant 17 °C in August and 9 °C in November. Regardless of the month of the test, the outlet water temperature decreased as the flow rate increased: the maximum outlet water temperature was 42 °C (flow rate equal to 0.25 L/min) and 22 °C (flow rate equal to 1.50 L/min) in August and 25 °C (flow rate equal to 0.25 L/min) and less than 15 °C (flow rate equal to 1.50 L/min) in November. The experimental results showed slight fluctuations caused by the experimental conditions and device uncertainties. The authors reported that

the trends predicted by the model and the experimental values obtained from the tests are in line, stating that the small deviations between the trends are due to the assumptions made in the development of the model.

As the intention of this review is to briefly summarize the latest works in massive solar collectors, in the Appendix A, the reader can find a complete table that gathers more information regarding the technological and thermal characteristics of these thermal storage systems (Table A1). In particular, the main parameters that play an important role in the final efficiency of these systems are shown, such as the geometric characteristics of the massive component, pipe characteristics (materials, diameters, and spacing), the fluid flow rate, and the type of final application.

### 3. Numerical Modeling

The modeling of MSTC can be simplified by following the assumptions proposed in the works of D'Antoni and Saro [3,5]. The first one is to consider that the temperature distribution between the tubes is the same, this allows us to represent the collector as a parallelepiped with a single tube and with a width that corresponds to the pitch between tubes. The second assumption is that the temperature gradient in a perpendicular plane to the fluid's path is considered greater than in a longitudinal one, allowing the MSTC to be divided in  $n$  sections in where the fluid's temperature is assumed constant. If  $n$  is increased, the accuracy of the model is consequently improved. The final aims of all these simplifications is to convert a three-dimensional problem into a two-dimensional one, which of course is less-expensive to solve. In this way, the temperature distribution  $T$  in the 2D domain  $\Omega$  of Figure 2 representing the collector can be obtained by solving Equation (1)

$$\rho c_{\text{eff}} \frac{\partial T}{\partial t} - \nabla \cdot (\mathbf{k} \nabla T) = 0 \quad \forall \mathbf{x} \in \Omega, \quad (1)$$

with  $\rho c_{\text{eff}}$  as the so-called effective heat capacity [19], which can be temperature-dependent in the presence of latent-based TES systems and can vary with the position vector  $\mathbf{x}$  of the domain  $\Omega$ ,  $t$  is the time, and  $\mathbf{k}$  is the (effective) thermal conductivity tensor of the material, which can also depend on the temperature  $T$  and vary throughout  $\mathbf{x}$ . Equation (1) is subject to the initial condition

$$T(\mathbf{x}, t) = T_0, \quad (2)$$

and the following boundary conditions:

$$\mathbf{k} \nabla T \cdot \mathbf{n}_1 = \dot{Q}_e, \quad (3)$$

$$\mathbf{k} \nabla T \cdot \mathbf{n}_2 = \dot{Q}_b, \quad (4)$$

$$\mathbf{k} \nabla T \cdot \mathbf{n}_3 = \dot{Q}_w, \quad (5)$$

$$\mathbf{k} \nabla T \cdot \mathbf{n}_4 = 0, \quad (6)$$

with  $\dot{Q}_e$  being the heat flux exchanged with the environment,  $\dot{Q}_b$  the one exchanged with the building, and  $\dot{Q}_w$  the one exchanged with the water. As said above, if the properties of the collector depend on the temperature, the Equation (1) becomes non-linear. Moreover, this non-linearity is stronger if the absorber material is combined with latent-based TES systems. For instance, when PCMs are present, the high non-linearity is due to the peaks that appear in the heat capacity when the phase change is developed. To model this behavior, the finite element formulation proposed by Morgan et al. [20] is adopted by Peralta et al. [8], where a robust solver is implemented to solve Equation (1). Another challenge for the modeling is to consider the collector working for a whole year, which will, in particular, allow us to

evaluate the device in periods of low radiation. In this sense, the boundary conditions of Equation (3) change hour by hour following the typical meteorological year (TMY) of the location where the MSTC is located, increasing the computational cost of the analysis.

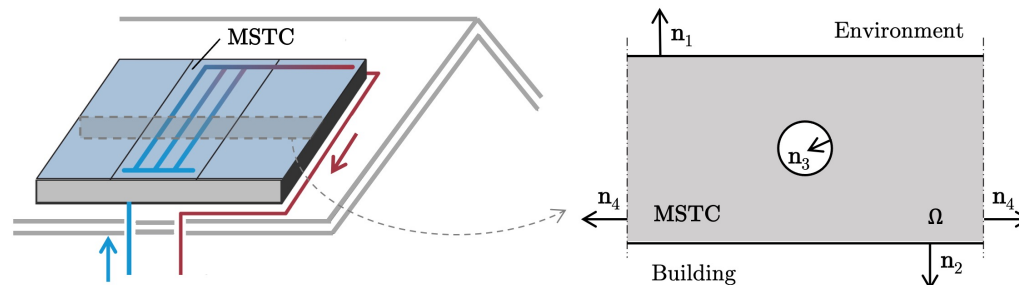


**Figure 2.** Sketch of a MSTC (left) and its 2D simplified domain of analysis (right). The water enters at the bottom (blue arrow), and leaves the collector at a higher temperature (red arrow).

Concerning the boundary condition of Equation (3), the heat flux exchanged with the environment is composed by many contributions. The main component is the absorbed short-wave radiation, which includes the direct and diffuse part. Another component is the heat flux exchanged with the sky and the ground by means of long-wave radiation. Then, there are two components of sensible and latent heat exchanged with the environment by means of convection and condensation of water over the collector, respectively. The contribution of evaporation to the exchanged latent heat can be neglected since its effect is not considerable [21]. For further details of how to calculate all the components, the reader should refer to the following works [5,8,11,13,17].

Regarding the heat flux exchanged with the building, in the case of detached configurations of the MSTC, or just to simplify the modeling, it can be assumed to be null as done by many authors [5,8,22]. For attached configurations, a convective boundary condition between the back of the collector and the indoor can be imposed. The envelope can be the collector itself or a sandwich structure composed by the collector, insulation and plaster, among other things. An example of this analysis has shown that this configuration of the collector could be useful to cool down a building during summer, while at the same time can allow for the extraction of useful energy [11].

In regards to the heat flux exchanged with the water, it could be considered by simply imposing a convection boundary condition between the wall of the tubes and the fluid [23], by assuming an imposed heat flux that can be obtained by a simple energy balance between the inlet and outlet temperatures of the fluid within the system [5], by considering the uncoupled solutions of the fluid and the solid part of the domain [13], which allows to transfer the information of the fluid's velocity field into the boundary of the solid domain representing the tubes, or by solving a fully couple problem in where the velocity field is calculated in the fluid domain, and the temperature field in both the fluid and the solid part of the collector [11].

As it is explained above, the modeling of an MSTC can be done in different ways, from simple 2D models up to complete, fully 3D simulations, which of course improves the accuracy at the expense of increasing the computational cost of solving these problems. The latest works regarding the modeling of solar collectors and the main outcomes of these works are summarized in the following paragraphs.

In the work of Sarachitti et al. [23] was proposed a mathematical model in which the conservation equations of energy are used to predict the performance of a roof-integrated solar concrete collector, i.e., no movement of the fluid is simulated. The model performed well since there is reasonable agreement between measured and predicted data. This type of attached collector showed a reduction in the heat gains into the building while, at the same time, a production of hot water. Another key point of the work is that the payback period for this system is only 2.54 years, an important characteristic for improving the market's penetration of this technology.

D'Antoni and Saro [5] studied the energy potential of considering the use of exposed concrete structures as devices to collect solar energy in European climates. A sensitivity analysis was performed to understand the relation between the design parameters of the solar collector and the energy output of the system. It was found that the diameter of the tubes, the spacing between them, and the absorber thickness are the main design parameters that influence the collector's energy output.

A finite element model developed by Guldentops et al. [13] was implemented in COMSOL Multiphysics to predict the behavior of a pavement solar collector. Particularly in this work, the flow was assumed to be uncoupled from the thermal problem (a good assumption in the presence of laminar flow). In this way, two different solvers were used, one for solving the laminar flow in stationary case (the fluid within the tubes), and another to solve the temperature field in the solid part of the collector (the pavement). Experimental data was used to validate the model and good agreements were found regarding the outlet temperatures of the fluid and pavement one. The main outcome of the work is that the asphalt thermal conductivity, surface absorptivity, and pipe depth are the most important parameters.

In the work of Tanzer and Schweigler [24] it was shown how industrial buildings façades can be exploited as a source of heat for heat pump heating devices. Opaque parts of the buildings were used as solar thermal collectors where the collected heat in summer is stored to be used in the heating seasons. The performance of the system was evaluated by using the modeling software TRNSYS 17. It was found that the main aspect for the correct functioning of the system is the sizing of the solar collector and the storage system.

O'Hegarty et al. [22] proposed a 2D finite element model (experimentally validated) of a solar collector, which is implemented in COMSOL Multiphysics. The 3D concrete collector was simplified by a 2D section, which is based on the fact that the temperature gradient in a perpendicular plane to the flow direction is significantly higher than in a parallel one, as assumed by D'Antoni and Saro [3,5]. Individual parameters that characterize the collector were evaluated to study their effect on the performance of the system. As a result of the study, concrete conductivity, and solar absorptance were pointed out as two important parameters that influence the performance of the device. A modification of these properties can increase the efficiency by 10% and 33%, respectively. In this sense, thermal conductivity can be increased by adding highly conductive materials, like metallic scrap and wire mesh, which have been shown to improve the performance of the collector [9].

Following the previous work, O'Hegarty et al. [11] developed a complete 3D finite element model in COMSOL Multiphysics to simulate a vertically installed concrete solar collector. It was considered a heat transfer problem coupled with the internal fluid flow. The model was also validated with experimentally measured data. The analyses showed that solar absorptance, the flow rate of the water, the pipe length, and the collector surface have an important influence on the performance of the system. It was also highlighted that in the presence of a well-insulated back of the concrete absorber, the collector has a negligible influence on the interior environment. This is an important point that allows us to simplify the modeling of solar collectors in general by assuming detached configurations.

Prakash [25] simulated an insulated roof system with a solar water heater. The flowing of the water inside the tubes was also calculated by computational fluid dynamics simulations (CFD) in Fluent software. Additionally, the model was validated with experimental results.

In the study of Zaim et al. [17], a CFD numerical model in ANSYS FLUENT was implemented to study the performance of pipe configurations of pavement solar collectors. The movement of the fluid inside the tubes and the heat exchange with the collector was considered. The main outcome of the work is that the parallel configuration for the tubes attains the best performance.

Masoumi et al. [18] analyzed the behavior of an asphalt solar collector by combining CFD analysis, validation with experimental data, and an artificial neural network (ANN) model. The whole system (collector, surrounding soil, and environment) was modeled by

using a finite volume method implemented in ANSYS CFX. The domain of analysis is a 3D model and the problem was solved in transient regime. Regarding the ANN model, it was used to perform a parametric study on all of the variables quantities together, with the aim of reducing the computational cost of considering all possible combinations. It was also found that improvements in the thermal conductivity and surface absorptivity of the asphalt have a positive effect in the daily performance of the system. Changing these properties can lead to an increase in the efficiency up to 6.4% and 12.2%, respectively.

Regarding the inclusion of latent-based TES systems in solar collectors, in the work of Benkaddour et al. [26], a finite volume element model was implemented to evaluate the effect of a paraffin wax PCM in different positions of a concrete-wall-integrated collector. It was found that as the PCM is moved away from the absorber in the wall, the stored latent heat in the paraffin wax becomes lower. In the work of Peralta et al. [8], an enthalpy-based finite element model was proposed to model the high non-linearity of the system as a consequence of the inclusion of PCMs within the absorber material of the collector. It was found that the correct inclusion of these latent-based TES materials can improve the energy performance of an MSTC. Improvements of 38.9% and 27.4% were possible in warm and cold climates, respectively. Furthermore, this work has studied the performance of the collector over a complete year and has considered the TYM of two different geographic locations. Again, for further reading, Table A1 in Appendix A can be consulted.

#### 4. Future Directions

As it is described in previous sections, the typical materials for solar collectors are concrete and asphalt. However, new research directions are devoted to finding new materials. In this sense, ceramic solar collectors seem to be an attractive alternative. Generally, they are made of typical ceramic raw materials, which include porcelain clay, quartz, and feldspar, among others, that own a certain degree of whiteness. To create an opaque absorber, a coating of V–Ti (vanadium-titanium) black ceramic is used, which allows us to obtain a solar absorptance in the range of 0.93–0.97 [27,28]. The main characteristic of ceramic solar collectors is their low cost, good thermostability, and long lifetime of the absorber material, which can be estimated at 100 years [29], this being an important parameter for the integration of these systems with the building. Another option for new materials is the use of greener cementitious materials, which are made of alkaline cement and hybrid cements. They can have better mechanical properties when they are exposed to high temperatures (in comparison with Portland cement mortars), and principally, they have improved thermal conductivity and specific heat [30,31], which nowadays allows us to use these materials as TES systems for concentrated solar power plants, and therefore could be a good alternative as absorber materials in MSTCs.

Regarding the improvement of the TES capacity of solar collectors, the use of PCMs for latent heat storage is gaining attention. The majority of the works done so far are in flat plate collectors, photo-voltaic solar collectors, and compound parabolic collectors; however, the main conclusions of these works could be extrapolated to MSTCs. In that sense, it was found that the outlet temperature of these systems can be enhanced if the contact area between the PCM and the absorber material is maximized [32]. Also, the common melting temperature of the used PCMs is around 52 °C, which is close to the discharging temperature of solar collectors (60 °C [33]). However, as it was stated by Chopra et al. [34], it is very important to study the economic viability of solar water heating systems with PCMs as the initial cost of the solar collector increases. In this regard, they studied the techno-economic benefits of solar collectors with and without PCMs, finding that systems with TES capabilities have interesting potential to obtain hot water at a cheaper rate. They compared both systems and concluded that those with PCMs have the lowest cost per liter of hot water, and also reduce the payback period from 4.12 to 3.56 years.

Following these ideas of applying PCMs in solar collectors, it was found that a smart inclusion of PCMs can improve the thermal energy performance of MSTCs [8], making this an interesting subject that has to be further explored. At the moment, three techniques of

PCM insertion are the most commonly used: micro-encapsulation, i.e., the insertion of the phase change material inside capsules that, in turn, are embedded in the cement matrix; in other cases, the phase change material forms a whole layer that is encapsulated in a container and inserted where it is needed; or the phase change material is encapsulated within the aggregates of the concrete.

About this last strategy of adding PCM, following [35], preliminary studies were conducted by the authors on the possibility of including PCMs directly within the pores of the aggregates that will later be used in the concrete mix design for the construction of the MSTC. At this preliminary stage, various aspects were considered for the selection of raw materials, including the final application, the maximum temperature that can be achieved with that type of collector, the possibility of using materials with a low environmental impact, and the final economic aspect of the prototype. Specifically, the recycled aggregate High porosity Poroton® fired-clay block (PB) was studied, and two paraffin waxes, RT 44 HC and RT 62 HC by Rubitherm Technologies GmbH, were selected as phase change materials, following the melting temperatures suitable for conventional solar collectors reported in [32]. The recycled aggregate was selected in order to keep the final cost low and to reuse materials that would otherwise cause further pollution through disposal processes. Regarding the PCMs, these paraffin waxes were chosen since they guarantee high thermal stability after numerous heating/cooling cycles. Moreover, these Rubitherm PCMs also have high specific heat capacity. The bricks were first crushed to obtain smaller particle sizes (Figure 3, left) and then, through mechanical sieving, the particle size distribution within the considered groups (0–0.5 mm, 0.5–1 mm, 1–2 mm, 2–4 mm, and 4–8 mm) was determined. In detail, mechanical sieving was carried out with an “AS 200 basic” vibrating plate from the company Retsch with a sieving time of 90 s per fraction and a frequency of 80 hertz. Sieve inserts with the following hole widths were used to determine the grain size curve: 16/8/4/2/1/0.5/0.25/0.125/0.063 mm (Figure 3, center). Once the Poroton® bricks had been crushed (Figure 3, left), they were first weighed and then, for each piece, three trays of 250 g each were prepared (statistical significance). The sample to be examined was passed through the series of sieves arranged in a column with a diameter decreasing from top to bottom, with the bottom closed by a lid to prevent the material from escaping (Figure 3, right). Once the column has been mechanically shaken, it was disassembled and the fraction of material retained by each individual sieve was weighed. This determines the weight of material passing through each individual sieve and relates it to the total weight of the sample. Figure 4 shows the particle size distribution curve of the analyzed sample of Poroton® bricks with, on the x-axis, the sieve opening in mm and, on the y-axis, the percentage by weight of the inert material passing through.



**Figure 3.** Experimental steps: (left) crushing aggregates; (center) cleaning sieves; (right) mechanical agitation of the aggregates.

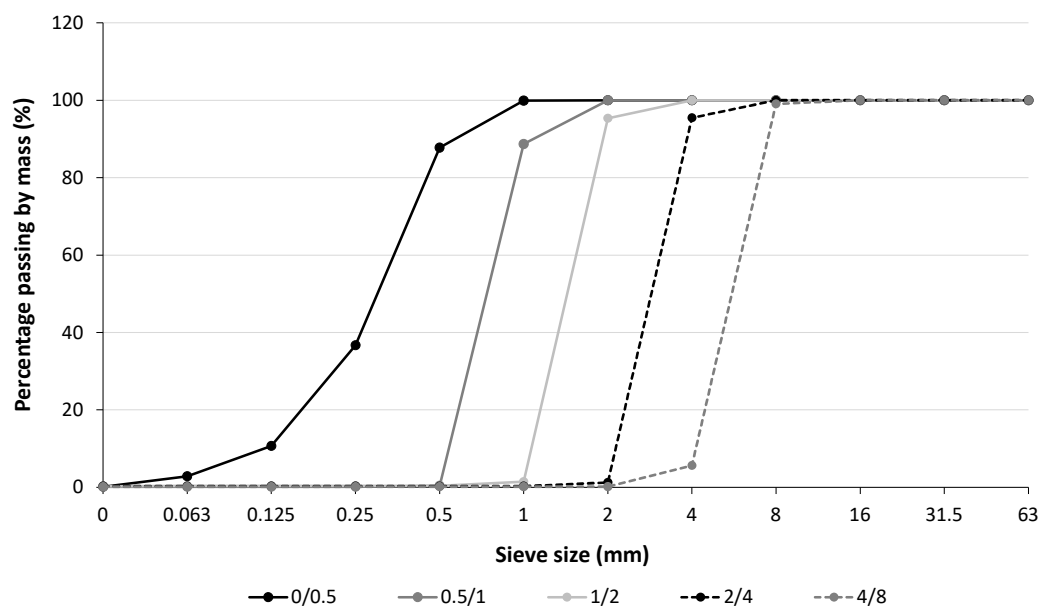


Figure 4. Characteristic curve of the recycled aggregate High porosity Poroton®.

Using a helium pycnometer, the density of the aggregates was determined, while the porosity of the aggregates was evaluated using the Mercury Intrusion Porosimetry (MIP) method following the standard procedure described in [36,37]. Table 1 shows the experimental results of the skeleton density for the six aggregate samples (three samples 2–4 mm and three samples 4–8 mm) together with the respective masses considered for each specimen. The average value of skeleton density was 2.637 g/cm<sup>3</sup>, while the value obtained for bulk density was 1.682 g/cm<sup>3</sup>. The results for the total porosity divided into closed and open pores obtained using the Hg-Porosimeter are shown in Table 2.

Table 1. Skeleton density of the Poroton® brick together with the relative masses considered for each sample.

Properties	Sample Identification Number					
	Sample 1 (2–4 mm)	Sample 2 (2–4 mm)	Sample 3 (2–4 mm)	Sample 1 (4–8 mm)	Sample 2 (4–8 mm)	Sample 3 (4–8 mm)
Sample skeleton density (g/cm <sup>3</sup> )	2.643	2.643	2.641	2.634	2.630	2.631
Sample mass (g)	0.839	0.637	1.247	1.008	1.128	1.101

Table 2. Total porosity of the Poroton® brick divided into closed and open pores.

Properties	Sample Identification Number					
	Sample 1 (2–4 mm)	Sample 2 (2–4 mm)	Sample 3 (2–4 mm)	Sample 1 (4–8 mm)	Sample 2 (4–8 mm)	Sample 3 (4–8 mm)
Open porosity (Vol.-%)	34.33	34.30	34.29	35.59	35.02	-
Closed porosity (Vol.-%)	2.95	1.64	1.78	0.45	0.79	-
Total porosity (Vol.-%)	37.28	35.94	36.07	36.04	35.81	-

Before filling the pores, all PB aggregates were completely dried in an oven (following the same methodology presented in [35]). Paraffin wax was introduced into the pores by spraying: the PCM was previously heated to a temperature of about 20 °C above its melting temperature and then, employing a spray gun, sprayed over the aggregates. For the PCM to permeate completely and homogeneously into the open capillary pores, manual agitation of the aggregates was applied. This procedure turned out to be very efficient and controllable (as shown also in [35]). Figure 5 shows the steps involved in filling the aggregates’ pores with the selected paraffin wax.



**Figure 5.** Experimental steps for filling aggregate pores: **(left)** pre-heating of the aggregate sample and paraffin wax in an electric oven; **(center)** weighing and spraying of paraffin respecting the calculated quantities; **(right)** manual agitation of the aggregates.

Table 3 shows the preliminary results obtained from the tests performed with the various instruments. In particular, the skeleton and bulk average density, the average volume percentage of the open and closed porosity, and the capillary pores of the aggregates are shown together with the required masses of paraffin wax as a function of the desired filling ratio considering the density in the liquid state of the paraffin. Achieving a filling ratio of 80% means that approximately close to 27% of the aggregates' volume can contain PCM, allowing an increment in the TES capacity of the material. In this way, it can be stated that the use of recycled aggregates can contribute positively in two ways, by increasing the TES capacity of the collector by using PCMs, and by reducing the negative environmental impact of construction and demolition wastes.

**Table 3.** Poroton® brick properties average results of MIP together with the required masses of the two paraffin waxes as a function of the desired filling degree. Quantities marked with \* refer to the data sheet provided by the manufacturer.

Properties	Value			
Skeleton density (g/cm <sup>3</sup> )	2.637			
Bulk density (g/cm <sup>3</sup> )	1.682			
Open porosity (Vol.-%)	34.706			
Closed porosity (Vol.-%)	1.522			
Total porosity (Vol.-%)	36.228			
Capillarity pores (Vol.-%)	94.394			
	RT 44 HC		RT 62 HC	
Paraffin liquid density * (g/cm <sup>3</sup> )	0.70		0.84	
Heat storage capacity * (kJ/kg)	250		230	
Filling degree (Vol.-%)	65	80	65	80
Amount of Paraffin (M.-%)	8.86	10.91	10.64	13.09

## 5. Conclusions

The objective of this review is to summarize significant aspects regarding the current state of development of massive solar thermal collector (MSTC) technologies, and the focus is mainly on the latest works after 2012. The main novelty of this review is to also provide a detailed summary of all the works completed so far in the field of MSTCs over the last 30 years, which are detailed in a simple table and can guide the searching of information regarding these type of solar devices. After explaining the latest main works done so far, the following can be itemized:

- MSTCs are simple devices to build and are easy to operate. They can be implemented as modular systems with reduced construction costs compared to the costs required to construct traditional collectors and are also easy to maintain. For instance, these reduced costs make these devices suitable for rural or remote areas where there is not always a supply of electricity.
- The durability of metallic materials of traditional flat solar collectors is limited by the threat of corrosion. Concrete, instead, is inherently durable, maintenance-free, and has good thermal storage qualities, which make this material an excellent candidate for MSTCs.
- Attention should be paid to the main parameters of MSTCs. In this sense, the thickness of the plate affects the performance of the collector. As the thickness of the collector increases, the efficiency factor and heat removal rate increase around 47% and 39%, respectively. Also, as the diameter of the tubes increases the fin effectiveness of the collector increases between 4% and 8.9%. On the contrary, as the space between the pipes increases the heat removal values decrease around 30% and 55%, whatever the plate thickness.
- There is a linear correlation between the solar collector area and hot water consumption. The integration of massive collectors in façades could be a good solution when there is a high demand for hot water but a small roof area of the building.
- The modeling of an MSTC can be done in different ways, from simple 2D models up to complete, fully 3D simulations, which of course improves the accuracy at the expense of increasing the computational cost of solving these problems. Finite element and finite volume methods are generally used to solve the physical problem. Additionally, artificial neural network models were also implemented to reduce the computational cost of the simulations.
- Simulation analyses showed that attached collectors (integrated with the façade) can reduce the heat gains into the building while at the same time producing hot water. Another key point is that the payback period for these systems is only 2.54 years, an important characteristic for improving the market's penetration of this technology.
- Sensitivity analysis by numerical modeling confirmed that the diameter of the tubes, the spacing between them, and the absorber thickness are the main design parameters that influence the collector's energy output, as was also demonstrated by experimental studies.
- Other studies showed that concrete thermal conductivity and solar absorptance are also pointed out as two important parameters that influence the performance of the device. Modification of these properties can increase the efficiency by 10% and 33%, respectively. In this sense, thermal conductivity can be increased by adding highly conductive materials, like metallic scrap and wire mesh, which have been shown to improve the performance of the collector.
- Using asphalt as an alternative material to concrete showed that thermal conductivity and asphalt surface absorptivity are also important parameters for MSTCs. Changing these properties can lead to an increase in efficiency up to 6.4% and 12.2%, respectively.
- Regarding the integration with buildings, it was found that in the presence of a well-insulated back of the concrete absorber material, the collector has a negligible influence on the interior environment of a building. This is an important point that allows us to simplify the modeling of solar collectors in general by assuming detached configurations.
- Regarding the inclusion of TES systems in solar collectors it was found that the correct inclusion of latent-based TES materials can improve the energy performance of MSTCs. Improvements of 38.9% and 27.4% were possible in warm and cold climates, respectively.

- The use of recycled aggregates could be an interesting choice for the use in MSTCs. They can contribute positively in two ways, by increasing the TES capacity of the collector by using PCMs, and by reducing the negative environmental impact of construction wastes.

According to everything discussed above, it can be concluded that MSTC technologies can contribute to the reduction of greenhouse gases and they are at the same time excellent examples of the integration of solar energy devices with the building envelope.

**Author Contributions:** Conceptualization, A.A. and I.P.; methodology, A.A. and I.P.; formal analysis, A.A. and I.P.; investigation, A.A. and I.P.; resources, E.A.B.K. and G.D.N.; data curation, A.A.; writing—original draft preparation, A.A. and I.P.; writing—review and editing, all authors; visualization, A.A. and I.P.; project administration, E.A.B.K. and I.P.; funding acquisition, E.A.B.K., I.P. and G.D.N. All authors have read and agreed to the published version of the manuscript.

**Funding:** This research was funded by the NRG-STORAGE project (870114, 2020–2024, <https://nrg-storage.eu/> (accessed on 9 August 2023)), financed by the European Union H2020 Framework under the LC-EEB-01-2019 call, IA type; the project Computational design of metamaterials applied to the development of thermal diodes for building envelopes (PICT 2020 SERIE A 03765) financed by the National Agency for the Promotion of Research, Technological Development and Innovation (AGENCIA) of Argentina.

**Data Availability Statement:** The data presented in this study are available in the Appendix A.

**Acknowledgments:** The first author is thankful for the Postdoc funds granted by Marche Polytechnic University (UNIVPM).

**Conflicts of Interest:** The authors declare no conflict of interest. The funders had no role in the design of the study; in the collection, analyses, or interpretation of data; in the writing of the manuscript; or in the decision to publish the results.

## Abbreviations

The following abbreviations are used in this manuscript:

CO <sub>2</sub>	Carbon dioxide
MSTC	Massive solar thermal collector
TES	Thermal Energy Storage
PCM	Phase Change Material
DHW	Domestic hot water
PVC	Polyvinyl chloride
PSC	Pavement solar collector
MFRC	Metal-fiber-reinforced concrete
ASC	Asphalt solar collector
TMY	Typical meteorological year
CFD	Computational fluid dynamics
ANN	Artificial neural network
MIP	Mercury Intrusion Porosimetry
PB	Poroton® fired-clay block
HDPE	High density polyethylene
PE-X	Polyethylene
GRC	Glass-reinforced concrete
CCC	Cellular-clayey concrete

## Appendix A

The following table provides a detailed summary of the works done so far in the field of MSTCs over the last 30 years.

**Table A1.** Main literature works on massive solar thermal collector (T = theoretical, E = experimental, W = water heating, DHW = domestic hot water, H = space heating, HR = heat reduction (effect of heat-island in a city), HT = heat transfer, HEE = heat energy extraction, IM = ice and snow melting process,  $A$  = collector surface,  $t$  = collector thickness,  $\varnothing_{in}$  = pipes inner diameter,  $\varnothing_{out}$  = pipes outer diameter,  $\delta$  = space between pipes,  $\dot{q}$  = fluid flow rate).

Year	Analysis (T/E)	Application	Massive Material	Main Characteristics $A$ (m <sup>2</sup> ), $t$ (m)	Pipe Material	Main Characteristics $\varnothing$ (mm), $\delta$ (mm), $\dot{q}$ (L/min)	Efficiency (Yes/No) Glazing, Back Insulation, Black Paint	References
2023	E	HR	Asphalt	$A = 0.08, t = 0.05$	Copper	$\varnothing_{out} = 24.5, \delta = \text{only 1 pipe}, \dot{q} = -$	no, yes, no	[38]
2022	T	DHW	Concrete	$A = -, t = 0.127$	-	$\varnothing_{out} = 25.4, \delta = 165, \dot{q} = -$	no, no, no	[8]
2021	E	DHW	Concrete	$A = 2.24, t = 0.10$	Aluminum	$\varnothing_{out} = 12.5, \delta = -, \dot{q} = 0.24, 0.38 \text{ and } 0.50$	no, no, yes	[39]
2020	T and E	W	Asphalt mixture	$A = 1.2, t = 0.2$	Stainless steel	$\varnothing_{in} = 15.8, \delta = 110, \dot{q} = 0.4, 1.34, 0.98 \text{ and } 1.07$	no, no, no	[17]
2020	T and E	W	Asphalt	$A = 1.0, t = 0.062$	Galvanised steel	$\varnothing_{in} = 14.0, \delta = 117, \dot{q} = 0.25\text{--}1.50$	no, yes, no	[18]
2019	E	W	Asphalt	$A = 0.50, t = 0.05$	Copper	$\varnothing_{in} = 9.52, \delta = 50, \dot{q} = 1.20$	yes, yes, no	[40]
2019	E	W	Reinforced Concrete	$A = 2.0, t = 0.03$	-	$\varnothing_{out} = 12.7, \delta = 150, \dot{q} = 1.0$	yes, yes, yes	[16]
2018	T	DHW	Concrete and refractory carborundum brick	$A = 16.0, t = 0.23$	Copper	$\varnothing_{out} = 10.0\text{--}20.0, \delta = -, \dot{q} = 0.12\text{--}0.22$	no, yes, no	[25]
2018	E	W	Concrete	$A = 2.0, t = 0.03$	Copper	$\varnothing = 8.0, \delta = 80, \dot{q} = 0.33\text{--}0.75$	yes, yes, no	[15]
2017	T	DHW and H	Concrete	$A = 1.0, t = 0.08$	Copper	$\varnothing_{out} = 15.0, \delta = 50, \dot{q} = 0.30$	no, yes, yes	[22]
2017	T and E	DHW	Concrete	$A = 1.0, t = 0.08$	Copper	$\varnothing_{out} = 15.0, \delta = 50, \dot{q} = 1.20$	no, yes, yes	[11]
2017	E	DHW	Reinforced Concrete	$A = 2.0, t = 0.035$	Copper	$\varnothing_{out} = 10.0, \delta = 80, \dot{q} = 0.50$	yes, yes, yes	[14]
2017	E	W	Ceramic	$A = 1.597, t = 0.027$	Ceramic	$\varnothing_{in} = 17.0, \delta = 40, \dot{q} = 1.98, 2.34, 2.70$	yes, yes, yes	[29]
2016	T and E	W	Asphalt concrete	$A = 1.67, t = 0.119$	Copper	$\varnothing_{out} = 15.0, \delta = 457, \dot{q} = 1\text{--}4$	no, no, no	[13]
2016	T and E	H	Concrete	$A = 2.20, t = 0.07$	-	$\varnothing_{out} = 12.0, \delta = -, \dot{q} = 2.50$	no, yes, no	[24]
2016	E	SWH	Reinforced Concrete	$A = 2.0, t = 0.10$	Copper	$\varnothing_{out} = 12.0, \delta = 80, \dot{q} = 0.417$	yes, yes, yes	[12]
2014	E	W	Concrete with/without aluminum wire mesh and iron scraps	$A = 2.24, t = 0.10$	Aluminum and PVC	$\varnothing = 12.5, \dot{q} = 1.20$	no, no, yes	[9]
2013	T	W	Concrete	$A = 3.50, t = 0.127$	PE-X	$\varnothing_{out} = 25.4, \delta = 16.5, \dot{q} = 15\text{--}75$ (kg/h m <sup>2</sup> )	no, no, no	[5]
2013	T	H	Concrete	$A = -, t = 0.07$	-	$\varnothing = 16.0, \delta = 200, \dot{q} = -$	no, yes, no	[41]
2013	E	W	Asphalt concrete (upper and bottom layers)	$A = 0.104, t = 0.09$	Porous asphalt layer instead of embedded pipe network	$\varnothing = -, \delta = -, \dot{q} = -$	no, no, no	[42]
2012	E	W	Concrete	$A = -, t = 0.25$	Acrylic plastic	$\varnothing = -, \delta = -, \dot{q} = -$	no, no, yes	[43]
2011	T and E	H	Plaster	$A = 2.5\text{--}5, t = -$	PE	$\varnothing = -, \delta = -, \dot{q} = -$	no, yes, yes	[44]
2011	T and E	W	Concrete	$A = 5.75, t = 0.12$	PVC	$\varnothing_{out} = 25.4, \delta = 100, \dot{q} = -$	no, no, no	[23]
2011	T and E	IM	Asphalt concrete	$A = 2.7, t = 0.1$	Copper	$\varnothing_{out} = 20, \delta = 300, \dot{q} = 0\text{--}1$	no, yes, no	[45]
2011	E	HR	Asphalt	$A = 0.09, t = 0.15$	Copper	$\varnothing_{out} = 20, \delta = 100, \dot{q} = 0\text{--}2$	no, yes, no	[46]
2010	T and E	DHW	Concrete	$A = 2.0, t = 0.04$	Copper	$\varnothing_{out} = 14, \delta = 100, \dot{q} = 2.48$	yes, yes, yes	[47]

Table A1. Cont.

Year	Analysis (T/E)	Application	Massive Material	Main Characteristics $A$ (m <sup>2</sup> ), $t$ (m)	Pipe Material	Main Characteristics $\varnothing$ (mm), $\delta$ (mm), $\dot{q}$ (L/min)	Efficiency (Yes/No) Glazing, Back Insulation, Black Paint	References
2010	T	IM	Asphalt	$A = 0.72, t = 0.078$	-	$\varnothing_{out} = 20, \delta = 90-150, \dot{q} = 1.17, 1.33$ and $1.67$	no, no, no	[48]
2009	E	HEE	Asphalt concrete	$A = 0.09, t = 0.15$	Copper	$\varnothing_{out} = 20, \delta = 100, \dot{q} = 0-1$	no, yes, no	[49]
2008	E	IM	Concrete pavement	$A = 1, t = 0.3$	HDPE	$\varnothing_{out} = 25, \delta = 200, \dot{q} = <83$	no, yes, no	[50]
2007	T	DHW and H	Concrete	$A = 5.25, t = 0.229$	Copper	$\varnothing = 6.35, \delta = -, \dot{q} = 11.4-0.00016$	yes, yes, yes	[51]
2004	T	W and H	Concrete	$A = 1.16, t = 0.038$	PE	$\varnothing_{out} = 20, \delta = 19, \dot{q} = -$	yes, no, yes	[52]
2002	T and E	HT	Concrete	$A = 0.312, t = 0.10$	Not present	$\varnothing = -, \delta = -, \dot{q} = -$	no, yes, no	[53]
2000	E	DHW	Reinforced Concrete	$A = 1.06, t = 0.055$	Aluminum	$\varnothing_{out} = 19.0, \delta = 60, \dot{q} = 1.33-1.67$	no, no, yes	[7]
2000	T and E	H	CCC	$A = 1.88, t = 0.20$	-	$\varnothing = -, \delta = -, \dot{q} = 5.6$ and $9.0$	no, no, no	[21]
1994	E	W	Concrete	$A = 0.90, t = 0.050$	Galvanised steel	$\varnothing_{in} = 16.4, \delta = 100,$ $\dot{q} = 0.011, 0.022$ and $0.033$ (kg/s m <sup>2</sup> )	yes, yes, yes	[54]
			Concrete	$A = 0.90, t = 0.050$	Propyleneglycol	$\varnothing_{in} = 13.0, \delta = 100,$ $\dot{q} = 0.011, 0.022$ and $0.033$ (kg/s m <sup>2</sup> )	yes, yes, yes	
			Concrete	$A = 0.93, t = 0.050$	PVC	$\varnothing_{in} = 13.5, \delta = 100,$ $\dot{q} = 0.011, 0.022$ and $0.033$ (kg/s m <sup>2</sup> )	yes, yes, yes	
1992	T	W	GRC	$A = -, t = 0.020$	-	$\varnothing = 10.0, \delta = 40-100, \dot{q} = -$	no, no, no	[55]
1992	T	W	Cellular concrete	$A = 0.90, t = 0.035$	PVC	$\varnothing_{out} = 20.0, \delta = 60-150, \dot{q} = 0.60-1.20$	yes, yes, yes	[56]
1989	E	W	Cellular concrete	$A = 0.90, t = 0.035$	PVC	$\varnothing_{out} = 20.0, \delta = 60-150, \dot{q} = 0.60-1.20$	yes, yes, yes	[57]

## References

1. European Union. *Causes of Climate Change*; European Union: Maastricht, The Netherlands, 2021.
2. IEA. *Key World Energy Statistics (KWES)*; IEA: Paris, France, 2021.
3. D'Antoni, M.; Saro, O. Massive Solar-Thermal Collectors: A critical literature review. *Renew. Sustain. Energy Rev.* **2012**, *16*, 3666–3679. [[CrossRef](#)]
4. Kalogirou, S.A. Solar thermal collectors and applications. *Prog. Energy Combust. Sci.* **2004**, *30*, 231–295. [[CrossRef](#)]
5. D'Antoni, M.; Saro, O. Energy potential of a Massive Solar-Thermal Collector design in European climates. *Sol. Energy* **2013**, *93*, 195–208. [[CrossRef](#)]
6. International Energy Agency (IEA). *Energy Conservation in Building & Communities Systems (ECBCS). Annex 44—Integrating Environmentally Responsive Elements in Buildings*; Project Summary Report by Prof. Per Heiselberg (2012); IEA: Paris, France, 2012.
7. Chaurasia, P. Solar water heaters based on concrete collectors. *Energy* **2000**, *25*, 703–716. [[CrossRef](#)]
8. Peralta, I.; Fachinotti, V.D.; Koenders, E.A.; Caggiano, A. Computational design of a Massive Solar-Thermal Collector enhanced with Phase Change Materials. *Energy Build.* **2022**, *274*, 112437. [[CrossRef](#)]
9. Krishnavel, V.; Karthick, A.; Murugavel, K.K. Experimental analysis of concrete absorber solar water heating systems. *Energy Build.* **2014**, *84*, 501–505. [[CrossRef](#)]
10. O'Hegarty, R.; Kinnane, O.; McCormack, S. A Case for façade located solar thermal collectors. *Energy Procedia* **2015**, *70*, 103–110. [[CrossRef](#)]
11. O'Hegarty, R.; Kinnane, O.; McCormack, S.J. Concrete solar collectors for façade integration: An experimental and numerical investigation. *Appl. Energy* **2017**, *206*, 1040–1061. [[CrossRef](#)]
12. Patil, S.R.; Keste, A.A.; Sable, A.B. Investigation and development of liquid flat plate solar collector using concrete as absorber plate and its performance testing. *Int. J. Renew. Energy Res. (IJRER)* **2016**, *6*, 1212–1220.
13. Guldentops, G.; Nejad, A.M.; Vuye, C.; den bergh, W.V.; Rahbar, N. Performance of a pavement solar energy collector: Model development and validation. *Appl. Energy* **2016**, *163*, 180–189. [[CrossRef](#)]
14. Sable, A. Experimental and economic analysis of concrete absorber collector solar water heater with use of dimpled tube. *Resour.-Effic. Technol.* **2017**, *3*, 483–490.
15. Patil, S.R.; Lodha, R.; Keste, A. Concrete solar collector—an experimental investigation in solar passive energy. *Mater. Today Proc.* **2020**, *23*, 366–372. [[CrossRef](#)]
16. Al Hoqani, T.M.; Bhambare, P.S.; Kaithari, D.K. Solar Thermal Energy Utilization using Metal Fiber Reinforced Concrete (MFRC) Collector for Producing Hot Water in Sultanate of Oman. *Int. J. Innov. Technol. Explor. Eng. (IJITEE)* **2019**, *8*, 1335–1340. [[CrossRef](#)]
17. Zaim, E.H.; Farzan, H.; Ameri, M. Assessment of pipe configurations on heat dynamics and performance of pavement solar collectors: An experimental and numerical study. *Sustain. Energy Technol. Assess.* **2020**, *37*, 100635. [[CrossRef](#)]
18. Masoumi, A.P.; Tajalli-Ardekani, E.; Golneshan, A.A. Investigation on performance of an asphalt solar collector: CFD analysis, experimental validation and neural network modeling. *Sol. Energy* **2020**, *207*, 703–719. [[CrossRef](#)]
19. Lopez, J.P.A.; Kuznik, F.; Baillis, D.; Virgone, J. Numerical modeling and experimental validation of a PCM to air heat exchanger. *Energy Build.* **2013**, *64*, 415–422. [[CrossRef](#)]
20. Morgan, K.; Lewis, R.W.; Zienkiewicz, O.C. An improved algorithm for heat conduction problems with phase change. *Int. J. Numer. Methods Eng.* **1978**, *12*, 1191–1195. [[CrossRef](#)]
21. Marmoret, L.; Glouannec, P.; Douzane, O.; t'Kint de Roodenbeke, A.; Queneudec, M. Use of a cellular clayey concrete for a wall specially fitted with water pipes. *Energy Build.* **2000**, *31*, 89–95. [[CrossRef](#)]
22. O'Hegarty, R.; Kinnane, O.; McCormack, S.J. Parametric investigation of concrete solar collectors for façade integration. *Sol. Energy* **2017**, *153*, 396–413. [[CrossRef](#)]
23. Sarachitti, R.; Chotetanorm, C.; Lertsatitthanakorn, C.; Rungsiyopas, M. Thermal performance analysis and economic evaluation of roof-integrated solar concrete collector. *Energy Build.* **2011**, *43*, 1403–1408. [[CrossRef](#)]
24. Tanzer, B.; Schweigler, C. Façade-integrated Massive Solar-thermal Collectors Combined with Long-term Underground Heat Storage for Space Heating. *Energy Procedia* **2016**, *91*, 505–516. [[CrossRef](#)]
25. Prakash, D. Thermal analysis of building roof assisted with water heater and insulation material. *Sādhanā* **2018**, *43*, 30. [[CrossRef](#)]
26. Benkaddour, A.; Faraji, M.; Faraji, H. Numerical study of the thermal energy storage behaviour of a novel composite PCM/Concrete wall integrated solar collector. *Mater. Today Proc.* **2020**, *30*, 905–908. [[CrossRef](#)]
27. Yang, Y.; Wang, Q.; Xiu, D.; Zhao, Z.; Sun, Q. A building integrated solar collector: All-ceramic solar collector. *Energy Build.* **2013**, *62*, 15–17. [[CrossRef](#)]
28. Xu, J.; Yang, Y.; Cai, B.; Wang, Q.; Xiu, D. All-ceramic solar collector and all-ceramic solar roof. *J. Energy Inst.* **2014**, *87*, 43–47. [[CrossRef](#)]
29. Zukowski, M.; Woroniak, G. Experimental testing of ceramic solar collectors. *Sol. Energy* **2017**, *146*, 532–542. [[CrossRef](#)]
30. Ramón-Álvarez, I.; Sánchez-Delgado, S.; Peralta, I.; Caggiano, A.; Torres-Carrasco, M. Experimental Characterization and Modelling of Geopolymers and Hybrid Materials for Solar Thermal Energy. In *International RILEM Conference on Synergising Expertise towards Sustainability and Robustness of Cement-Based Materials and Concrete Structures*; Springer Nature: Cham, Switzerland, 2023; pp. 1176–1188. [[CrossRef](#)]

31. Ramón-Álvarez, I.; Sánchez-Delgado, S.; Peralta, I.; Caggiano, A.; Torres-Carrasco, M. Experimental and computational optimization of eco-friendly mortar blocks for high temperature thermal energy storage of concentrated solar power plants. *J. Energy Storage* **2023**, *71*, 108076. [\[CrossRef\]](#)
32. Khan, M.M.A.; Ibrahim, N.I.; Mahbulul, I.; Ali, H.M.; Saidur, R.; Al-Sulaiman, F.A. Evaluation of solar collector designs with integrated latent heat thermal energy storage: A review. *Sol. Energy* **2018**, *166*, 334–350. [\[CrossRef\]](#)
33. Lee, T.; Hawes, D.; Banu, D.; Feldman, D. Control aspects of latent heat storage and recovery in concrete. *Sol. Energy Mater. Sol. Cells* **2000**, *62*, 217–237. [\[CrossRef\]](#)
34. Chopra, K.; Tyagi, V.; Pandey, A.; Sharma, R.K.; Sari, A. PCM integrated glass in glass tube solar collector for low and medium temperature applications: Thermodynamic & techno-economic approach. *Energy* **2020**, *198*, 117238. [\[CrossRef\]](#)
35. Mankel, C.; Caggiano, A.; Koenders, E. Thermal energy storage characterization of cementitious composites made with recycled brick aggregates containing PCM. *Energy Build.* **2019**, *202*, 109395. [\[CrossRef\]](#)
36. Scrivener, K.; Snellings, R.; Lothenbach, B. *A Practical Guide to Microstructural Analysis of Cementitious Materials*; CRC Press: Boca Raton, FL, USA, 2018.
37. Berodier, E.; Bizzozero, J.; Muller, A.C. Mercury intrusion porosimetry. In *A Practical Guide to Microstructural Analysis of Cementitious Materials*; CRC Press: Boca Raton, FL, USA, 2016; Volume 419.
38. Abbas, F.A.; Alhamdo, M.H. Thermal performance of asphalt solar collector by improving tube and slab characteristics. *Int. J. Thermofluids* **2023**, *17*, 100293. [\[CrossRef\]](#)
39. Chandrika, V.; Karthick, A.; Kumar, N.M.; Kumar, P.M.; Stalin, B.; Ravichandran, M. Experimental analysis of solar concrete collector for residential buildings. *Int. J. Green Energy* **2021**, *18*, 615–623. [\[CrossRef\]](#)
40. Pukdum, J.; Phengpom, T.; Sudasna, K. Thermal performance of mixed asphalt solar water heater. *Int. J. Renew. Energy Res.* **2019**, *9*, 712–720.
41. Karabay, H.; Arıcı, M.; Sandık, M. A numerical investigation of fluid flow and heat transfer inside a room for floor heating and wall heating systems. *Energy Build.* **2013**, *67*, 471–478. [\[CrossRef\]](#)
42. Pascual-Muñoz, P.; Castro-Fresno, D.; Serrano-Bravo, P.; Alonso-Estébanez, A. Thermal and hydraulic analysis of multilayered asphalt pavements as active solar collectors. *Appl. Energy* **2013**, *111*, 324–332. [\[CrossRef\]](#)
43. Bellamy, L.A. An experimental assessment of the energy performance of novel concrete walls embedded with mini solar collectors. *Energy Procedia* **2012**, *30*, 29–34. [\[CrossRef\]](#)
44. Ruschenburg, J.; Baisch, K.; Oltersdorf, T.; Courtot, F.; Herkel, S. Experimental and Simulation Results on a Solar-Assisted Heat Pump Prototype for Decentral Applications. In Proceedings of the IEA 10th Heat Pump Conference 2011, Tokyo, Japan, 27 June–31 August 2011; Volume 16.
45. Chen, M.; Wu, S.; Wang, H.; Zhang, J. Study of ice and snow melting process on conductive asphalt solar collector. *Sol. Energy Mater. Sol. Cells* **2011**, *95*, 3241–3250. [\[CrossRef\]](#)
46. Shaopeng, W.; Mingyu, C.; Jizhe, Z. Laboratory investigation into thermal response of asphalt pavements as solar collector by application of small-scale slabs. *Appl. Therm. Eng.* **2011**, *31*, 1582–1587. [\[CrossRef\]](#)
47. Hazami, M.; Kooli, S.; Lazâar, M.; Farhat, A.; Belghith, A. Energetic and exergetic performances of an economical and available integrated solar storage collector based on concrete matrix. *Energy Convers. Manag.* **2010**, *51*, 1210–1218. [\[CrossRef\]](#)
48. Gao, Q.; Huang, Y.; Li, M.; Liu, Y.; Yan, Y. Experimental study of slab solar collection on the hydronic system of road. *Sol. Energy* **2010**, *84*, 2096–2102. [\[CrossRef\]](#)
49. Wu, S.; Chen, M.; Wang, H.; Zhang, Y. Laboratory study on solar collector of thermal conductive asphalt concrete. *Int. J. Pavement Res. Technol.* **2009**, *2*, 130–136.
50. Wang, H.; Zhao, J.; Chen, Z. Experimental investigation of ice and snow melting process on pavement utilizing geothermal tail water. *Energy Convers. Manag.* **2008**, *49*, 1538–1546. [\[CrossRef\]](#)
51. Hassan, M.M.; Beliveau, Y. Design, construction and performance prediction of integrated solar roof collectors using finite element analysis. *Constr. Build. Mater.* **2007**, *21*, 1069–1078. [\[CrossRef\]](#)
52. Abbott, A. Analysis of Thermal Energy Collection form Precast Concrete Roof Assemblies. Master’s Thesis, Virginia Polytechnic Institute and State University, Blacksburg, VA, USA, 2004.
53. Bilgen, E.; Richard, M.A. Horizontal concrete slabs as passive solar collectors. *Sol. Energy* **2002**, *72*, 405–413. [\[CrossRef\]](#)
54. Al-Saad, M.; Jubran, B.; Abu-Faris, N. Development and testing of concrete solar collectors. *Int. J. Sol. Energy* **1994**, *16*, 27–40. [\[CrossRef\]](#)
55. Sokolov, M.; Reshef, M. Performance simulation of solar collectors made of concrete with embedded conduit lattice. *Sol. Energy* **1992**, *48*, 403–411. [\[CrossRef\]](#)
56. Bopshetty, S.; Nayak, J.; Sukhatme, S. Performance analysis of a solar concrete collector. *Energy Convers. Manag.* **1992**, *33*, 1007–1016. [\[CrossRef\]](#)
57. Nayak, J.; Sukhatme, S.; Limaye, R.; Bopshetty, S. Performance studies on solar concrete collectors. *Sol. Energy* **1989**, *42*, 45–56. [\[CrossRef\]](#)

**Disclaimer/Publisher’s Note:** The statements, opinions and data contained in all publications are solely those of the individual author(s) and contributor(s) and not of MDPI and/or the editor(s). MDPI and/or the editor(s) disclaim responsibility for any injury to people or property resulting from any ideas, methods, instructions or products referred to in the content.